ARCHIVES OF ACOUSTICS
8, 1, 11-30 (1983)

DETECTABILITY OF GAS BUBBLES IN BLOOD BY THE ULTRASONIC METHOD

LESZEK FILIPCZYŃSKI

Department of Ultrasound, Institute of Fundamental Technological Research,
Polish Academy of Sciences
(00-049 Warsaw, ul. Świętokrzyska 21)

The reflection of a plane ultrasonic wave from a gas bubble in the blood was considered quantitatively in the range $ka \leqslant 1$ (a is the radius of the bubble, $k = 2\pi/\lambda$ and λ is the wavelength). Taking as an example the elbow vein (vena basilica), the losses in a signal caused by electroacoustical transducing, attenuation of the wave in tissues, reflection of the wave from the bubble and divergence of the reflected wave were evaluated using a typical ultrasonic Doppler device with a frequency of 8 MHz.

It was shown that a single gas bubble with the radius 1.6 μm already gives a signal which is received by the device; this signal, however, is masked by the signal caused by the scattering of the wave by blood cells and, in addition, this bubble is instable. Determination of the level of signals scattered in blood indicated that in the case investigated it is possible to detect in the vein a single gas bubble with its radius greater than 16 μm or gas bubbles with a radius of 11 μm lying at the stability limit provided that their density exceeds 35 cm^{-3}.

The present calculation procedure permits the determination in a specific anatomic case of the level of signals scattered by blood, the level of electronic noise and also the determination of the detectability of gas bubbles in blood caused, for example, by the decompression of divers or by the caisson disease. In the case of the pulmonary artery, using a frequency of 5 MHz, minimum radii of detectable gas bubbles greater than 70 μm were obtained.

Notation

A — surface area of the transducer
A_l — attenuation loss
a — radius of the gas bubble
a_d — radius of the gas bubble lying at the detectability limit
a_0 — limiting radius of the gas bubble
a_m — expansion coefficient of the wave reflected from the gas bubble
$\bar{a}_m$ — expansion coefficient of the wave penetrating into the gas bubble

a_t — radius of the transducer
B — level of the signal scattered by blood cells
c — wave velocity in blood
$\bar{c}$ — wave velocity in gas
$\bar{c}_0$ — wave velocity in gas under normal conditions
c^D — wave velocity in the transducer with constant electric induction
c_A — wave velocity in the medium loading the back surface of the transducer
c_B — wave velocity in the medium loading the front surface of the transducer
D — loss caused by the divergence of the ultrasonic beam
d — internal diameter of the blood vessel
d_t — thickness of the transducer
e — base of natural logarithms
f — frequency
f_e — frequency of electromechanical resonance in the transducer
f_m — frequency of mechanical resonance in the transducer
f_{res} — resonance frequency of the gas bubble
$h_m^{(2)}$ — spherical Hankel function of the second kind of order m
$h_m^{(2)\prime}$ — see formula (5a)
I_0 — intensity of the plane incident wave
I_s — intensity of the scattered spherical wave
$J_{m+1/2}$ — Bessel function of order $m+1/2$
j — $\sqrt{-1}$
j_m — a spherical Bessel function of order m
j_m' — see formula (5b)
k — wave number in blood
$\bar{k}$ — wave number in gas
k_t — coefficient of electromechanical coupling
l — distance of the blood vessel from the transducer
M_s — scattering power
M_A — power emitted at the back loading of the transducer
M_B — power emitted at the front loading of the transducer (biological medium)
m — natural number
$N_{m+1/2}$ — Neuman function of order $m+1/2$
n_m — spherical Neuman function of the order m
n — density of blood cells (erythrocytes)
n_0 — density of gas bubbles
P_m — Legendre polynomial (spherical function)
P_a — static pressure of air
P_l — static pressure in liquid
P_i — static pressure in a gas bubble
P_δ — static pressure caused by the surface tension
p_i — static pressure of the incident wave
p_0 — acoustic pressure amplitude of the incident wave
p_s — acoustic pressure of the reflected (scattered) wave
R — reflection loss
r — radial coordinate of the polar system
S — loss caused by scattering in blood
T — loss caused by piezoelectric transducing
t — time
W — ratio of the maximum to the minimum electric signal
V — blood volume in the ultrasonic beam

v_A – velocity of the back surface of the transducer
v_B – velocity of the front surface of the transducer
x – relative frequency (see formula (19))
x_e – relative frequency of the electric resonance of the transducer
α_m – the scattering (intensity) coefficient in muscle tissue
α_b – the scattering (intensity) coefficient blood
Γ_ϑ – function of far field reflection
δ – equivalent cross-section of scattering by blood cells
η – coefficient of backscattering
θ – inclination angle of the ultrasonic beam
ϑ – angular coordinate of the polar system
λ – wavelength in blood
ϱ – density of blood
$\bar{\varrho}$ – density of gas
ϱ_0 – density of gas under normal conditions
ϱ_t – density of the transducer
ϱ_A – density of the medium loading the back surface of the transducer
ϱ_B – density of the biological medium loading the front surface of the transducer
Σ – equivalent cross-section of scattering of the gas bubble
Σ_0 – equivalent cross-section of scattering of a gas bubble with the limiting radius
σ – surface tension at the blood-air interface
ω – angular frequency

1. Introduction

Ultrasonic diagnostic methods permit the possibility of detecting such structures in the human body whose acoustic specific impedance is different from the impedance of the surrounding tissues. These are, for example, gas bubbles in divers' blood during decompresion (divers' or caisson disease) or in persons staying at high altitudes. An ultrasonic method permits detection of the presence of gas bubbles in blood even before distinct, clinical symptoms of this disease occur [20]. Gas bubbles in blood are also detected ultrasonically in the blood circulation system in the artificial kidney.

Gas bubbles in blood are detected by means of the ultrasonic Doppler technique [19, 20] and, in some applications, by means of the conventional pulse technique. In some of our investigations [15] performed in cooperation with the Central Institute of Occupational Safety, the Doppler technique was used at a frequency of 5 MHz to observe the appearance of gas bubbles in the pulmonary artery. SPENCER *et al.* [20], who were the first to use the method, showed that it was also possible to detect gas bubbles in the veins of the peripheral circulation system, e.g. in the elbow vein (vena basilica).

The principal aim of this investigation is to evaluate the minimum size of a single, spherical gas bubble to be detectable in blood using ultrasonic, Doppler or pulse, methods. The author found no answer to this problem in papers related to this subject [2, 10, 12, 19, 20]. A quantitative analysis of the

problem will be performed in the case of detection of gas bubbles in the elbow vein (vena basilica) using a Doppler method under the conditions shown in Fig. 1.

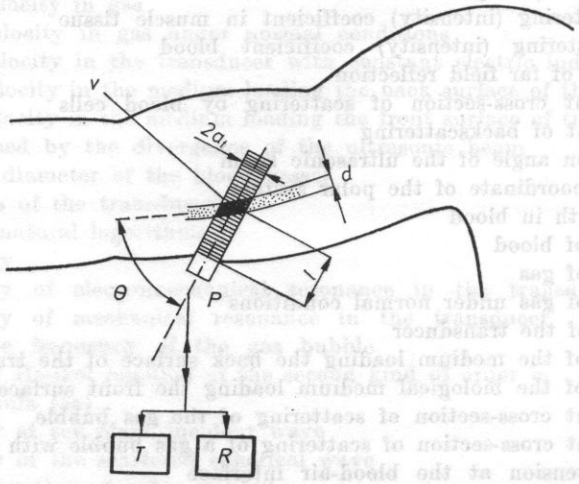

Fig. 1. The system for detection of gas bubbles in the elbow vein (vena basilica) P – the ultrasonic probe with a piezoelectric transducer, T – the transmitter of electric signals, R – the receiver of electric signals, d – the diameter of the vein, V – the volume of blood covered by the ultrasonic beam, l – the depth at which the vein lies, θ – the inclination angle of the ultrasonic beam with respect to the vein, $2\,a_t$ – the diameter of the ultrasonic beam

2. Assumptions of the analysis

It can be assumed that an ultrasonic beam of longitudinal waves at a frequency of 8 MHz is radiated by a piezoelectric transducer with the diameter $2a_t = 5$ mm. The mean wave velocity in soft tissues is approximately equal to the wave velocity in blood ($c = 1.57$ km/s). Thus the radiated wavelength is $\lambda = 0.2$ mm. The boundary between the near and the for field is then $a_t^2/\lambda = 31$ mm. Considering typical anatomic conditions, it can be assumed that the vein of interest with its internal diameter $d = 3$ mm lies at the depth $l = 15$ mm from the body surface on which the piezoelectric transducer was placed (Fig. 1). It can then be recognized that at this distance the ultrasonic beam is cylindrical. The mean (in the cross-section of the beam) wave intensity is, as a result of diffraction loss, lower by only about 1.5 dB at the distance l than at the body surface [3].

An ultrasonic Doppler device [5] will be used to detect gas bubbles. The output voltage of the transmitter is $U_T = 4$ V when matched to the impedance of the ultrasonic probe, i.e. 50 Ω. The voltage sensitivity of the receiver limited by electronic noise is $U_R = 4$ μV. Under these conditions the ratio of the maximum to the minimum electronic signal is $W = U_T/U_R = 10^6 \doteq 120$ dB.

3. Reflection of a plane ultrasonic wave from a gas bubble in blood

A further step of calculations here will be the determination of the acoustic pressure of the wave reflected from a spherical gas bubble with the radius a. It can be assumed additionally that the wave of the acoustic pressure incident on the gas bubble is plane. The reflection of the plane wave from a sphere filled with a fluid medium (liquid or gas) was considered in detail by RSHEVKIN in his monograph [16] and subsequently by MORSE and INGARD [11]. The further part of this paper is based on the former of these references.

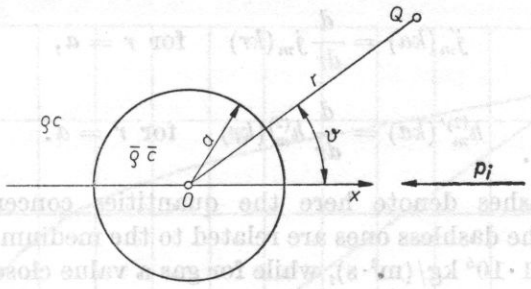

Fig. 2. The polar coordinate system (r, ϑ) with a gas bubble in the shape of a sphere with radius a and with a plane acoustic pressure wave p_i incident in the direction $-X$
ϱc, $\bar{\varrho} c$ are the acoustic specific impedance of the media, respectively, outside and inside the sphere

In a threedimensional polar coordinate system a plane continuous wave with the acoustic pressure p_i, incident in the negative direction of the x axis (Fig. 2) on a sphere placed at the origin of the system, can be represented as an infinite series of spherical waves of the form [16]

$$p_i = p_0 \exp(j\omega t) \sum_{m=0}^{\infty} j^m (2m+1) P_m(\cos\vartheta) j_m(kr). \tag{1}$$

The wave reflected from the sphere can, in turn, be expressed in the form of an infinite series of spherical waves propagating in the medium surrounding the sphere in the direction of the increasing radius r

$$p_s = \exp(j\omega t) \sum_{m=0}^{\infty} a_m P_m(\cos\vartheta) h_m^{(2)}(kr). \tag{2}$$

The wave penetrating into the sphere can be described by the expression

$$p_t = \exp(j\omega t) \sum_{m=0}^{\infty} \bar{a}_m P_m(\cos\vartheta) j_m(\bar{k}r). \tag{3}$$

The coefficients a_m and $\bar{a}_m$ are determined from the boundary conditions satisfied on the surface of the sphere $(r = a)$ which are the continuity of the acoustic pressure and of the radial component of the acoustic velocity on the

surface of the sphere. RSHEVKIN gives the following expression for the expansion coefficients [16]

$$a_m = -p_0 j^m (2m+1) \frac{j'_m(ka) - \frac{\varrho c}{\bar{\varrho}\bar{c}} \frac{j'_m(\bar{k}a)}{j_m(\bar{k}a)} j_m(ka)}{h_m^{(2)\prime}(ka) - \frac{\varrho c}{\bar{\varrho}\bar{c}} \frac{j_m(\bar{k}a)}{j'_m(\bar{k}a)} h_m^{(2)}(ka)}, \tag{4}$$

where

$$j'_m(ka) = \frac{d}{dr} j_m(kr) \quad \text{for } r = a, \tag{5a}$$

$$h_m^{(2)\prime}(ka) = \frac{d}{dr} h_m^{(2)}(kr) \quad \text{for } r = a. \tag{5b}$$

Horizontal dashes denote here the quantities concerning the medium inside the sphere, the dashless ones are related to the medium outside the sphere. For blood $\varrho c = 1.61 \cdot 10^6$ kg/(m^2·s), while for gas a value close to that for air can be assumed, $\varrho c = 0.0004 \cdot 10^6$ kg/(m^2·s).

MORSE and INGARD [11] give analogous formulae in a slightly different form, which, it can readily be verified, are the same as RSHEVKIN's formulae.

The point of interest here is the wave reflected at the point Q (Fig. 2) at a distance so far from the centre of the sphere that the following condition is satisfied

$$r \gg \lambda \quad \text{or} \quad kr \gg 1. \tag{6}$$

Thus the Hankel function $h_m^{(2)}$ can be approximated by the expression

$$h_m^2(z) \underset{z\to\infty}{\to} \frac{1}{z} \exp\left[-j\left(kr - \frac{m+1}{2}\pi\right)\right]. \tag{7}$$

Considering formula (7) expression (2) becomes

$$p_s = p_0 \frac{\exp(-jkr)}{kr} \Gamma_\vartheta(ka), \tag{8a}$$

where

$$\Gamma_\vartheta(ka) = \sum_0^\infty a_m P_m(\cos\vartheta) \exp[j(m+1)\pi/2]. \tag{8b}$$

The quantity $\Gamma_\vartheta(ka)$ will be called the function of far field reflection. This function depends on the argument ka and on the angle ϑ (Fig. 2). However, in the ultrasonic technique used for detection of gas bubbles in blood one common piezoelectric transducer is used for transmission and detection of ultrasonic waves or two transducers placed in one probe close to each other. In

such a case only the value of the function $\Gamma_\vartheta(ka)$ in the direction of the wave radiation, i.e. for the angle $\vartheta = 0$, is of interest here. This simplifies further calculations, since for $\vartheta = 0$, $P_m(1) = 1$. Hence the function

$$\Gamma_{\vartheta=0}(ka) = \sum_0^\infty a_m \exp[j(m+1)\pi/2] \tag{9}$$

is only dependent on the argument ka. Fig. 3 shows this function calculated in the dB scale for low values of $ka = 0.05$-1.4. The values of the spherical

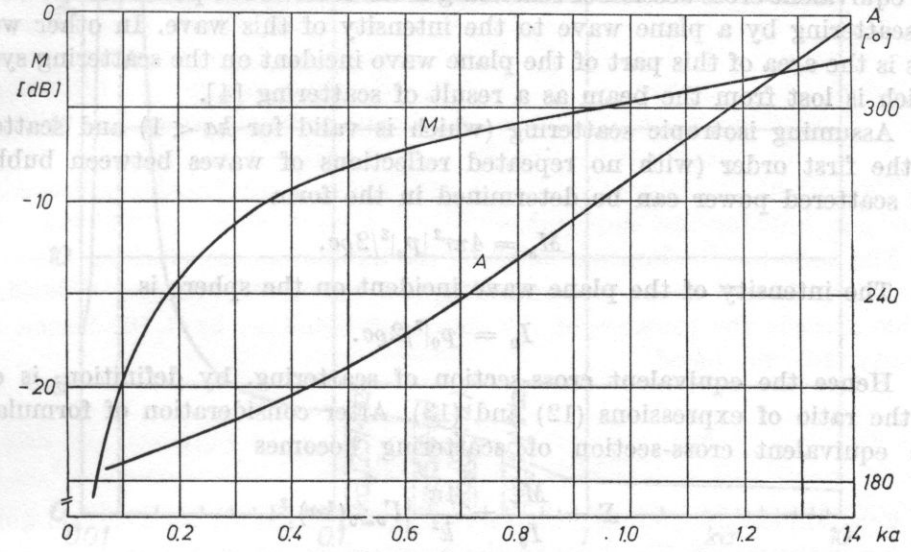

Fig. 3. The function of far field reflection $\Gamma_{\vartheta=0}$ (ka) from the gas bubble in blood ($\vartheta = 0$, $kr \gg 1$)

M – the mode $\Gamma_{\vartheta=0}$ (ka), A – arg $\Gamma_{\vartheta=0}$ (ka), a – the radius of the bubble, $k = 2\pi/\lambda$

functions necessary for the determination of the values of coefficients (4) were calculated from the following relations between these functions and the Bessel and Neuman functions of order 1/2

$$j_m(z) = \sqrt{\frac{\pi}{2z}}\, J_{m+\frac{1}{2}}(z), \tag{10a}$$

$$n_m(z) \sqrt{\frac{\pi}{2z}}\, N_{m+\frac{1}{2}}(z), \tag{10b}$$

$$h_m^{(2)}(z) = j_m(z) - j n_m(z). \tag{10c}$$

In turn, the values of the function $J_{m+1/2}(z)$ and $N_{m+1/2}(z)$ were calculated using the library of subprogrammes of a CYBER 70 IBM computer.

On the basis of the curve of the function $\Gamma_{\vartheta=0}(ka)$ and formula (8a), the pressure p_s of the wave reflected from a single gas bubble can be determined. The quantity

$$R = 20 \log \operatorname{mod} \Gamma_{\vartheta=0}(ka) \tag{11}$$

represents the loss in the signal caused by the reflection of the wave from the gas bubble.

In the case of a large number of bubbles it becomes practical to introduce the notion of the equivalent cross-section of scattering [4, 9]. By definition the equivalent cross-section of scattering is the ratio of the power lost as a result of scattering by a plane wave to the intensity of this wave. In other words, this is the area of this part of the plane wave incident on the scattering system which is lost from the beam as a result of scattering [4].

Assuming isotropic scattering (which is valid for $ka < 1$) and scattering of the first order (with no repeated reflections of waves between bubbles), the scattered power can be determined in the form

$$M_s = 4\pi r^2 |p_s|^2 / 2\varrho c. \tag{12}$$

The intensity of the plane wave incident on the sphere is

$$I_0 = |p_0|^2 / 2\varrho c. \tag{13}$$

Hence the equivalent cross-section of scattering, by definition, is equal to the ratio of expressions (12) and (13). After consideration of formula (8), the equivalent cross-section of scattering becomes

$$\Sigma = \frac{M_s}{I_0} = \frac{4\pi}{k^2} |\Gamma_{\vartheta=0}(ka)|^2. \tag{14}$$

The function $\Gamma_\vartheta(ka)$ was determined only for the value of the angle $\vartheta = 0$ and therefore expression (14) is valid strictly for consideration of backscattered signals in the incidence direction of the plane wave. For $\vartheta \neq 0$ this formula becomes approximate, to be used when $ka < 1$.

It is interesting to note the ratio of the equivalent cross-section of scattering Σ to the cross-section area of the bubble πa^2, shown as a function of ka in a broad range of this product in Fig. 4. The curve calculated shows a maximum for the value $ka_{\text{res}} \approx 0.014$, which corresponds to resonance vibrations of the bubble; these vibrations are of the zeroth order. The value of this maximum depends on the magnitude of energy of the reflected wave, viscosity of the surrounding liquid and on the thermal conduction of the liquid [10].

Neglecting in first approximation the viscosity of the liquid and also the surface tension, the resonance frequency of the bubble can be determined from the formula [16]

$$f_{\text{res}} = \frac{1}{2\pi a} \sqrt{\frac{3\bar{\varrho}\bar{c}_0^2}{\varrho} \frac{P_l}{P_0}}, \tag{15}$$

where ϱ_0 and c_0 denote respectively the density and wave velocity in gas under normal conditions (temperature 0°C, normal pressure $P_0 = 750$ mm Hg $= 1000$ hPa).

The above formula assumes an adiabatic transition of gas in the bubble. In the case of very small bubbles, as a result of low gas volume and high thermal conduction of the liquid, the phenomenon is isothermal and the above formulae require some modification [10]. This, however, does not cause any greater change in the resonance frequency.

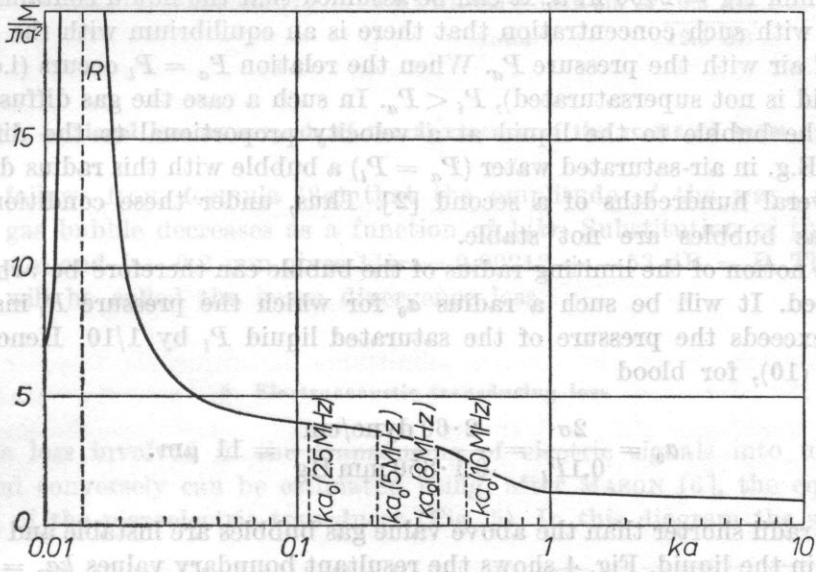

Fig. 4. The relative equivalent cross-section of backscattering of the gas bubble in blood calculated in relation to ka from formulae (14), (9) and (4)

Σ – the absolute equivalent cross-section of backscattering; a, a_0 and a_{res} – respectively, the radius, the limiting radius and the resonance radius of the gas bubble, R – the vibration resonance of the bubble

Attention should be drawn to the phenomenon of the surface tension occurring on the surface of the gas bubble. It causes the appearance of additional pressure directed from the liquid to the surface of the bubble. This pressure has the value [8]

$$P = \frac{2\sigma}{a}. \tag{16}$$

The surface tension of blood has the value $\sigma = 60$ dyne/cm [12]. For a bubble radius longer than 10 μm, from formula (16), the pressure P_σ caused by this is lower by almost one order of magnitude than the mean blood pressure in man which is taken as 850 mm Hg $= 1.13 \cdot 10^5$ dyne/cm^2 $= 1130$ hPa.

In the case of gas bubbles with shorter diameters the pressure within the bubble becomes greater than that of the surrounding liquid, since the following equation occurs [2],

$$P_i = P_1 + \frac{2\sigma}{a}, \tag{17}$$

where P_i is the gas pressure inside the bubble and P_l is the static pressure in the liquid. For $a = 0.5$ μm the excessive value of this pressure is $P_i - P_l = 1800$ mm Hg $= 2400$ hPa. It can be assumed that the liquid contains dissolved gas with such concentration that there is an equilibrium with the gaseous phase of air with the pressure P_a. When the relation $P_a = P_l$ occurs (i.e. when the liquid is not supersaturated), $P_i < P_a$. In such a case the gas diffuses from within the bubble to the liquid at a velocity proportional to the difference $P_i - P_a$. E.g. in air-saturated water ($P_a = P_l$) a bubble with this radius dissolves over several hundredths of a second [2]. Thus, under these conditions very small gas bubbles are not stable.

The notion of the limiting radius of the bubble can therefore be arbitrarily introduced. It will be such a radius a_0 for which the pressure P_i inside the bubble exceeds the pressure of the saturated liquid P_l by 1/10. Hence, from formula (10), for blood

$$a_0 = \frac{2\sigma}{0.1P_l} = \frac{2 \cdot 60 \text{ dyne/cm}}{0.1 \cdot 850 \text{ mm Hg}} = 11 \text{ μm}. \tag{18}$$

For radii shorter than the above value gas bubbles are instable and quickly dissolve in the liquid. Fig. 4 shows the resultant boundary values $ka_0 = 2\pi f a_0/c$ for frequencies $f = 2.5$, 5, 8 and 10 MHz. It follows therefore that no practical possibility exists for resonance to occur when bubbles are detected using frequencies equal to or higher than 2.5 MHz.

It follows from Fig. 4 that in the range $ka = 0.11\text{-}10$ the equivalent cross-section of scattering is from 4 to 1 times as large as the area of the equatorial cross-section of the gas bubble.

4. Signal loss as a result of wave attenuation in the biological medium

Evaluation of the attenuation of ultrasonic waves on their way from the body surface through the skin, muscle and the wall of a blood vessel to its interior can only be approximate. Table 1 presents such an evaluation. Considering the path of an ultrasonic wave in both directions, attenuation loss can be taken as $A_l = -25$ dB.

Table 1. Estimation of ultrasonic wave attenuation on the path from the transducer to the vessel (vena basilica) (extrapolated for the frequency $f = 8$ MHz)

1. Muscle (including skin) (acc. to HOETER [7])	9.0 dB cm^{-1} · 1.3 cm =	11.7 dB
2. Vessel wall (acc. to GREENLEAF [7])	4.8 dB cm^{-1} · 0.1 cm =	0.5 dB
3. Blood (acc. to KIKUCHI [7]	2.2 dB cm^{-1} · 0.15 cm =	0.3 dB
	total	12.5 dB

5. Signal loss as a result of the divergence of the scattered beam

It follows from formula (8*a*) that the amplitude of the wave reflected from a gas bubble decreases as a function of $1/kr$. Substitution of the values $r = 15$ mm and $\lambda = 0.2$ mm gives $1/kr = 0.00212 \doteq -53$ dB $= D$. The quantity D will be called the beam divergence loss.

6. Electroacoustic transducing loss

The loss involved in the transducing of electric signals into ultrasonic ones and conversely can be estimated using, after MASON [6], the equivalent system of the piezoelectric transducer (Fig. 5). In this diagram the symbol x

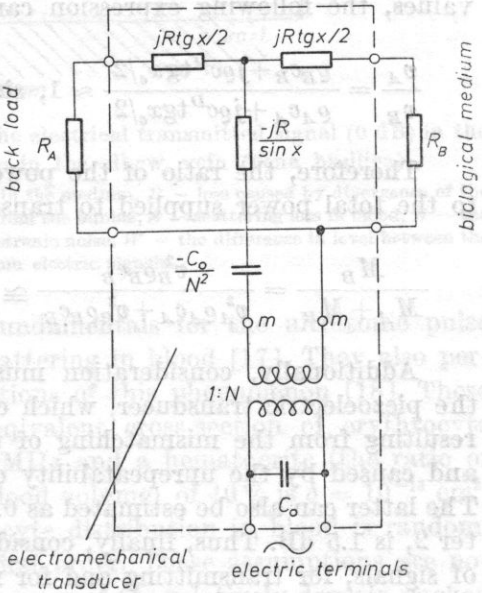

Fig. 5. The equivalent electromechanical system of the piezoelectric transducer with thickness vibration, according to MASON

$R_A = A\varrho_A c_A$, $R_B = A\varrho_B c_B$, $R = A\varrho_t c^D$, A – the surface area of the transducer, C_0 – the static capacity of the transducer, N – the "turn" ratio of the electromechanical transformer, x – the relative frequency

denotes the relative frequency equal to

$$x = \pi f/f_m = \omega d/c^D. \tag{19}$$

With good enough approximation it can be assumed that [6]

$$f_e/f_m = \sqrt{1-k_t^2}\,. \tag{20}$$

Taking for the ceramic material CERAD used here the value of the coefficient of electromechanical coupling for thickness vibration $k_t = 0.5$ and the frequency of electromechanical resonance $f_e = 8$ MHz, the following value can be obtained from formulae (19) and (20),

$$x_e = \pi\sqrt{1-k_t^2} = 2.72. \tag{21}$$

On the basis of the equivalent diagram (Fig. 5), the simple relation can be written

$$v_A(\varrho_A c_A + j\varrho c^D \operatorname{tg} x_e/2) = v_B(\varrho_B c_B + j\varrho c^D \operatorname{tg} x_e/2). \tag{22}$$

Measurements of the electric admittance of ultrasonic Doppler probes used in the continuous wave blood flow measurements give the value of the acoustic impedance $\varrho_A c_A = 3\cdot 10^6$ kg/(m^2·s). The acoustic specific impedance of soft tissues has the average value $\varrho_B c_B = 1.6\cdot 10^6$ kg/(m^2·s). The analogous value for piezoelectric transducers is greater by an order of magnitude and varies within the limits $\varrho c^D = (25\text{-}35)\cdot 10^6$ kg/(m^2·s). Considering the above values, the following expression can be derived from formula (22),

$$\frac{v_A}{v_B} = \frac{\varrho_B c_B + j\varrho c^D \operatorname{tg} x_e/2}{\varrho_A c_A + j\varrho c^D \operatorname{tg} x_e/2} \approx 1, \text{ since } \quad \varrho_B c_B < \varrho_A c_A \ll \varrho c^D \operatorname{tg} x_e/2. \tag{23}$$

Therefore, the ratio of the power M_B emitted in the biological medium to the total power supplied to transducer is

$$\frac{M_B}{M_A + M_B} = \frac{v_B^2 \varrho_B c_B}{v_A^2 \varrho_A c_A + v_B^2 \varrho_B c_B} \cong \frac{\varrho_B c_B}{\varrho_A c_A + \varrho_B c_B} = 0.35 \doteqdot -4.6 \text{ dB}. \tag{24}$$

Additionally, consideration must be given to the loss occurring inside the piezoelectric transducer, which can be estimated as 0.75 dB, and the loss resulting from the mismatching of the transducers to the electronic systems and caused by the unrepeatability of the parameters of ceramic transducers. The latter can also be estimated as 0.75 dB. The diffraction loss, given in chapter 2, is 1.5 dB. Thus, finally, considering the double piezoelectric transducing of signals, for transmitting and for receiving of signals, the total transducing loss $T = -15$ dB can be determined.

7. Wave scattering in blood

Fig. 6 shows all the signal losses which have been calculated so far. Under the measurement conditions assumed the smallest gas bubble at the detectability limit would be a bubble for which $ka = 0.05$. This corresponds to the radius $a = 0.05\lambda/2\pi = 1.6$ μm; since then the signal received would be equal to the level of electronic noise N. It can be noted, however, that red blood cells (erythrocytes) have dimensions Ø 8.5 ×2.5 μm. Moreover, aggregates of blood cells up to 6-10 cells, or sometines up to hundreds of cells, form in large blood vessels [5]. Accordingly, it is essential to explain to what extent the wave scattering, mostly by erythrocytes, masks the signal from a single gas bubble.

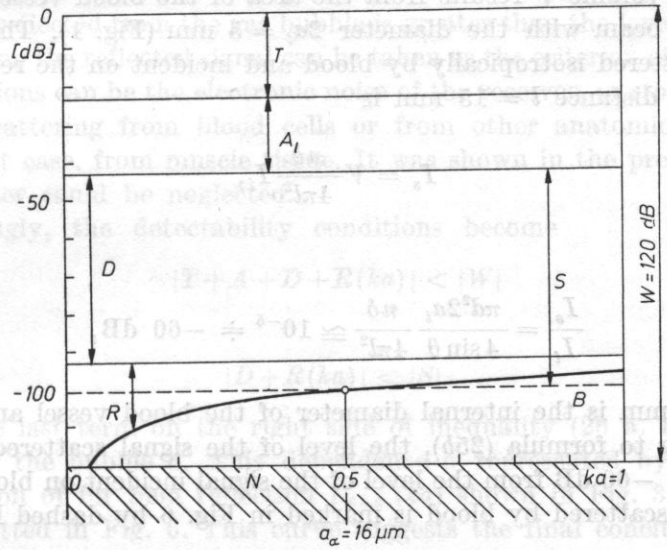

Fig. 6. The level of the signals with respect to the electrical transmitted signal (0 dB) in the course of the detection of a gas bubble in the elbow vein (vena basilica)

T – piezoelectric transducing loss, A_l – attenuation loss in the medium, D – loss caused by divergence of the beam scattered by bubbles, R – loss caused by reflection from the bubble, S – scattering loss in blood, B – the level of the signal scattered in blood, N – the level of electronic noise, W – the difference in level between the maximum and minimum electric signals

Reid *et al.* developed theoretical fundamentals for the ultrasonic pulse method for the measurement of wave scattering in blood [17]. They also performed extensive experimental investigations of this phenomenon [18]. These authors determined the value of the eqivalent cross-section of erythrocyte scattering which for a frequency of 8.5 MHz and a hematocrite (the ratio of the volume of erythrocytes to the total blood volume) of 40 % is $\delta = 10^{-13}$ cm^2.

It can be assumed that the erythrocyte distribution in blood is random, while the reflection is isotropic, of the first order. These assumptions are not strictly satisfied in blood, for example, because of the relatively densely packed

erythrocytes. As the packing density of erythrocytes (increasing hematocrite) increases, the equivalent cross-section of scattering decreases [17]. Multiple reflection might occur then or the erythrocyte distribution might cease to be random. The scattering phenomenon becomes more complicated; despite this, a single model of scattering can be used, taking the above assumptions for satisfied. The argument for this assumption is the fact that the amplitude of each successive wave reflected from an erythrocyte is lower by at least 23 dB than the amplitude of the previous reflected wave. This results from the hardly distinct difference in acoustic specific impedance between erythrocyte and blood plasma [5].

The erythrocyte density $n = 5 \cdot 10^6$ mm^{-3} can now be assumed. The scattering blood volume V results from the area of the blood vessels covered by an ultrasonic beam with the diameter $2a_t = 5$ mm (Fig. 1). The intensity of the wave scattered isotropically by blood and incident on the receiving transducer at the distance $l = 15$ mm is

$$I_s = V \frac{n\delta}{4\pi l^2} I_i, \tag{25a}$$

hence

$$\frac{I_s}{I_i} = \frac{\pi d^2 2a_t}{4 \sin\theta} \frac{n\delta}{4\pi l^2} \cong 10^{-6} \doteq -60 \text{ dB}, \tag{25b}$$

where $d = 3$ mm is the internal diameter of the blood vessel and $\theta = 45°$.

According to formula (25*b*), the level of the signal scattered by blood is lower by $S = -60$ dB from the level of the signal incident on blood. The level of the signal scattered by blood is marked in Fig. 6 by dashed line *B*.

8. Wave scattering in muscle tissue

The scattering of ultrasonic waves in muscle tissue is much greater than that in blood. This can be shown on the basis of the results of experimental investigations performed on the muscles of dog's hearts by O'DONNOLL *et al.* [14]. At a frequency of 8 MHz they determined the value of the differential coefficient of backscattering $\eta = 2.5 \cdot 10^{-2}$ cm$^{-1} \cdot$sr^{-1}. Therefore, assuming isotropic scattering, the (intensity) coefficient of scattering [4] is $a_m = 4\pi\eta$ cm^{-1} $= 0.32$ cm^{-1}. In turn, the analogous scattering coefficient for blood is $a_b = \delta n = 5 \cdot 10^{-4}$ cm^{-1}. Thus, when the scattering volumes of muscle and blood, placed at the same distance from the transmit-receive transducer, are assumed to be the same, the power of the signal scattered in muscle is greater by $a_m/a_b = 640 \doteq 28$ dB than that of the signal scattered in blood.

However, in contrast to blood, muscle tissue or, alternatively, other tissues penetrated by ultrasonic wave is stationary. Accordingly, the wave scattered by this tissue does not change its frequency with respect to the incident wave; the Doppler phenomenon is absent. In view of this, the signals of these waves can be eliminated electronically, e.g. by filtration or the technique of stationary echo cancellation [13].

9. Detectability of gas bubbles

The radius of the gas bubble detectable by means of the present method can be determined directly from Fig. 6. The condition for which the magnitude of the signal reflected from the gas bubble is greater than the level of disturbing signals masking the reflected signal can be taken as the criterion of detectability. These distortions can be the electronic noise of the receiver, or stochastic signals caused by scattering from blood cells or from other anatomical structures; in the present case, from muscle tissue. It was shown in the preceding section that the latter could be neglected.

Accordingly, the detectability conditions become

$$|T+A+D+R(ka)| < |W| \tag{26a}$$

and

$$|D+R(ka)| < |S|. \tag{26b}$$

Only the last term on the right side of inequality (26 a, b) depends on the radius of the bubble a. This dependence is represented by the modulus of the function of far field reflection $\Gamma_{\vartheta=0}(ka)$ shown in Fig. 3 (see formula (11)) and plotted in Fig. 6. This curve suggests the final conclusion that the detectability condition (26) is satisfied for a single gas bubble for which $ka > 0.5$. For a frequency of 8 MHz used here this signifies that the radius of the bubble detectable under the present conditions must satisfy the condition

$$a > a_d = 0.5\frac{\lambda}{2\pi} = 16\mu\text{m}. \tag{27}$$

In the case of a larger number of gas bubbles in blood the situation becomes complicated insomuch as the distribution of the size of bubbles with different radii is not known. Therefore, the least convenient detectability conditions are taken, under the assumption that only gas bubbles with limiting radii (lying at the stability limit) whose radius was determined by formula (18), occur in blood.

The density n_0 [cm^{-3}] of such bubbles, necessary for their detection, can then be found. At a frequency of 8 MHz the equivalent cross-section of scattering of a bubble with the boundary radius $a_0 = 11$ μm is $\Sigma_0 = 3\pi a_0^2$ (see Fig. 4),

while for a single bubble lying at the detectability limit, with the radius $a_d = 16\ \mu m$ ($ka = 0.5$), this value is $\Sigma = 2.5\pi a_d^2$. The power of the signal reflected from $n_0 V$ bubbles with the radius a_0, equal to $I_i \Sigma_0 n_0 V$, can be equated to the power of the signal reflected from a single gas bubble with the radius a_d, equal to $I_i \Sigma$. Hence, the desired density of bubbles follows,

$$n_0 = \frac{\Sigma}{\Sigma_0 V} = \frac{2.5\pi a_d^2}{3\pi a_0^2} \frac{4 \sin\theta}{\pi d^2 2a_t} \cong 35\ \text{cm}^{-3}. \tag{28}$$

The analysis performed indicates that the sensitivity of the method for detection of gas bubbles is very large, since they are detectable with density as low as 35 cm^{-3}. Calculations were made for air bubbles, while divers' work involves nitrogen bubbles. The wave velocity and the density of nitrogen and air differ from each other by only a few percent [1, 8]; and therefore the results obtained can be extended to the case of nitrogen bubbles.

The above procedure for the calculation of the detectability of bubbles can be used with success in the case of other blood vessels. As an example, the detectability of bubbles in the pulmonary artery can now be calculated. This is an important case from the practical point of view, because of the fact that all the blood in the circulation system flows through this artery, when one neglects the slight bronchial flow. By covering the entire cross-section of the pulmonary artery with the ultrasonic beam, it is possible to control fully the circulation.

A disadvantage of this measurement system is the higher attenuation of signals in view of the greater depth of the pulmonary artery, compared to the case of the veins in the peripheral system, and also in view of the movements of the heart which make examination more difficult.

It is now possible to take an ultrasonic beam and a pulmonary artery with diameters of 1.3 cm and the centre of the artery at the depth $l = 4$ cm. Table 2 shows the estimation of loss as a result of attenuation in the penetrated tissue. It follows from this table that attenuation on the path from the transducer to the centre of the pulmonary artery and back is $A = -48$ dB.

Table 2. Estimation of ultrasonic wave attenuation on the path from the transducer to the pulmonary artery (extrapolated for the frequency $f = 8$ MHz)

1. Muscle (including skin)	9.0 dB $cm^{-1} \cdot 1$ cm = 9 dB
2. Adipose and connective tissue	6 dB $cm^{-1} \cdot 2$ cm = 12 dB
3. Vessel wall	5 dB $cm^{-1} \cdot 0.2$ cm = 1 dB
4. Blood (to the centre of the artery)	2.2 dB $cm^{-1} \cdot 0.8$ cm = 1.8 dB
	total 23.8 dB $\cong$ 24 dB

The loss resulting from the divergence of the scattered ultrasonic beam is, according to formula (8a), $D = 20 \log 0.2 \text{ mm}/2\pi \cdot 40 \text{ mm} = -62$ dB (see section 5). The total loss $T+A+D = -125$ dB is so great that, even when neglecting the reflection loss $R(ka)$, the signal received would be lower than the level of electronic noise of the device, and thus undetectable. For this reason it is necessary to eliminate the frequency of 8 MHz from further consideration and to use instead a frequency of 5 MHz, also typical of Polish-made Doppler equipment.

Since attenuation in soft tissue is directly proportional to frequency, attenuation loss then decreases to the value $A = 30$ dB. The loss caused by the divergence of the scattered beam is $D = 20 \log 0.32 \text{ mm}/2\pi \cdot 40 \text{ mm} = -58$ dB.

The level of the signal scattered by blood also changes to become

$$S = I_s/I_i = V \frac{n\delta}{4\pi l^2} = -60 \text{ dB},$$

where $V = 2.2$ cm^3 is the blood volume in the artery covered by the ultrasonic beam ($a_t = 7.5$ mm) and $\delta = 2 \cdot 10^{-14}$ cm^2 is the equivalent cross-section of scattering of erythrocyte for a frequency of 5 MHz [18]. The detectability condition (26b) becomes $|-58 \text{ dB} + R(ka)| < |-60 \text{ dB}|$, hence the inequality $R(ka) > -2$ dB results. Considering relation (11), the value $ka = 1.4$ can be found for $R(ka) = -2$ dB from the curve in Fig. 3. It follows therefore that at a frequency of 5 MHz single gas bubbles with a radius greater than $a_d = 70$ μm can be detected.

10. Conclusions

The analysis and calculations performed here show that in the anatomical case considered (elbow vein – vena basilica), when a typical ultrasonic Doppler device is used at a frequency of 8 MHz, even a single gas bubble with a radius greater than 1.6 μm gives a signal received by an electronic device. This signal, however, is masked by signals caused by wave scattering in blood. Moreover, the bubble with so small a radius is unstable. The level of the signals scattered in blood (B in Fig. 6) is equal to the level of the signal from a single gas bubble with a radius of 16 μm ($ka = 0.5$). Thus single gas bubbles with a radius greater than 16 μm are detectable. Bubbles with a minimum radius of 11 μm lying at the stability limit are detectable when their density exceeds 35 cm^{-3}.

In the case of the pulmonary artery the frequency of the ultrasonic wave should be decreased in view of the overlarge attenuation in tissue. It was shown that when a frequency of 5 MHz is used, single gas bubbles with radii greater than 70 μm are detectable.

It is interesting to note that this is the necessary but not sufficient detectability condition, since detection of a signal above the level of distortions requires some difference between these levels and the probability of detection of gas bubbles increases as this difference increases.

The values of the radius and density of detectable gas bubbles obtained here depend on dimensions and position of the blood vessel in which measurements are taken, on the kind of tissue penetrated by the ultrasonic beam and on the electronic and acoustic parameters of the ultrasonic equipment used.

For simplification it was assumed in the present analysis that the acoustic pressure distribution in the near field of the ultrasonic beam was uniform and equal to the mean value for the beam cross-section. In practice local minima and maxima of the acoustic pressure occur in the beam; these maxima being theoretically twice as large as the mean value mentioned. This value can cause variations in the signal received from the gas bubbles as it crosses with the blood flow the successive minima and maxima in the beam.

The present calculation procedure permits the estimation in a specific case of the detectability of gas bubbles in blood and also the estimation of the level of signals received from blood with respect to electronic noise of the device. This makes possible the optimization of the technological conditions of electronic and acoustic devices for investigations of blood flows and for detection of gas bubbles in blood.

The present calculations have to a large extent the nature of an estimation and therefore the results should be regarded as approximate. Although these results apply to continuous wave Doppler equipment, their extension to pulse equipment does not offer difficulties.

References

[1] J. BLITZ, *Fundamentals of ultrasonic*, Butterworths, London 1967.

[2] W. COAKLEY, W. NYBORG, *Cavitation; Dynamics of gas bubbles; Applications*, (Ultrasound, F. FRY, ed.), Part I, Chapter II, Elsevier, Amsterdam 1978, p. 79.

[3] B. FAY, *Numerische Berechung der Beugungsversluste im Schallfeld von Ultraschallwandlern*, Acustica, **36**, 209-213 (1976/77).

[4] L. FILIPCZYŃSKI, *Ultrasonic characterization of tissues in cardiology*, Archives of Acoustics, **8**, 1, 83-93 (1983).

[5] L. FILIPCZYŃSKI, R. HERCZYŃSKI, A. NOWICKI, T. POWAŁOWSKI, *Blood flows — hemodynamics and ultrasonic Doppler measurement methods* (in Polish), PWN, Warsaw 1980.

[6] L. FILIPCZYŃSKI, G. ŁYPACEWICZ, *Dependence between the Q-value of piezoelectric transducers loaded acoustically and the electromechanical coupling coefficient*, Proceedings of Vibration Problems, Warsaw, **10**, 2, 213-229 (1969).

[7] S. GOSS, E. JOHNSTON, F. DUNN, *Comprehensive compilation of empirical ultrasonic properties of mammalian tissues*, J. Acoust. Soc. Am., **64**, 2, 423-457 (1978).

[8] GRIMSEHL TOMASCHEK, *Lehrbuch der Physik*, Band I. Teubner, Leipzig 1942, p. 269.

[9] I. MALECKI, *Theory of waves and acoustic systems*, PWN, Warsaw 1964.

[10] H. MEDWIN, *Counting bubbles acoustically: a review*, Ultrasonics, **15**, 1, 7-13 (1977).

[11] P. MORSE, K. INGARD, *Theoretical acoustics*, McGraw Hill, New York 1968, p. 425.

[12] R. NISHI, *Ultrasonic detection of bubbles with Doppler flow transducers*, Ultrasonics, 173-179 (July 1972).

[13] A. NOWICKI, J. REID, *Dynamic ultrasonic visualization of blood vessels and flows*, Archives of Acoustics, **7**, 3-4, 225-245 (1983).

[14] M. O'DONNOLL, J. MIMBS, J. MILLER, *Relationship between collagen and ultrasonic backscatter in myocardial tissue*, J. Acoust. Soc. Am., **69**, 2, 580-588 (1981).

[15] P. RUSZCZEWSKI, J. ETIENNE, A. NOWICKI, *A method for detection of gas bubbles in blood* (in Polish), Bezpieczeństwo Pracy, CIOP, Warsaw, **10**, 14-18 (1981).

[16] S. N. RSHEVKIN, *Lectures on theory of sound* (in Russian), Moscow 1960, p. 272.

[17] R. SIGELMANN, J. REID, *Analysis and measurement of ultrasound backscattering from an ensemble of scatterers excited by sinewave bursts*, J. Acoust. Soc. Am., **53**, 1351-1355 (1973).

[18] K. SHUNG, R. SIGELMANN, J. REID, *Scattering of ultrasound by blood*, IEEE Transactions on Biomedical Eng., **23**, 460-467 (1976).

[19] M. SPENCER, *Decompression limits for compressed air determined by ultrasonically detected blood bubbles*, J. Appl. Physiology, **40**, 2, 229-235 (1976).

[20] M. SPENCER, H. CLARKE, *Precordial monitoring of pulmonary gas embolism and decompression bubbles*, Aerospace Medicine, **43**, 7, 762-767 (1972).

Received on September 17, 1981; revised version on July 1, 1982.